Martin, P. G., Griffiths, I., Jones, C., Stitt, M., Davies-Milner, M., Mosselmans, JFW., Yamashiki, Y., Richards, D., & Scott, T. (2016). In-situ removal and characterisation of uranium-containing particles from sediments surrounding the Fukushima Daiichi Nuclear Power Plant. *Spectrochimica Acta Part B: Atomic Spectroscopy*, *117*, 1-7. https://doi.org/10.1016/j.sab.2015.12.010

Spectrochimica Acta Part B 117 (2016) 1–7

Contents lists available at ScienceDirect

Spectrochimica Acta Part B

journal homepage: www.elsevier.com/locate/sab

In-situ removal and characterisation of uranium-containing particles from sediments surrounding the Fukushima Daiichi Nuclear Power Plant

P.G. Martin [a,*], I. Griffiths [b], C.P. Jones [a], C.A. Stitt [a], M. Davies-Milner [c], J.F.W. Mosselmans [d], Y. Yamashiki [e], D.A. Richards [f], T.B. Scott [a]

[a] Interface Analysis Centre, HH Wills Physics Laboratory, University of Bristol, Bristol BS8 1TL, UK
[b] School of Physics, HH Wills Physics Laboratory, University of Bristol, Bristol BS8 1TL, UK
[c] School of Earth Sciences, Wills Memorial Building, University of Bristol, Bristol BS8 1RJ, UK
[d] Diamond Light Source, Harwell Science and Innovations Campus, Didcot, Oxfordshire OX11 0DE, UK
[e] Graduate School of Advanced Integrated Studies in Human Survivability, Kyoto University, Kyoto 606-8501, Japan
[f] Bristol Isotope Group, School of Geographical Sciences, Bristol BS8 1SS, UK

ARTICLE INFO

Article history:
Received 24 June 2015
21 December 2015
Accepted 23 December 2015
Available online 31 December 2015

Keywords:
Fukushima Daiichi
μ-XAS
Synchrotron
Radioactivity
Uranium

ABSTRACT

Traditional methods to locate and subsequently study radioactive fallout particles have focused heavily on autoradiography coupled with in-situ analytical techniques. Presented here is the application of a Variable Pressure Scanning Electron Microscope with both backscattered electron and energy dispersive spectroscopy detectors, along with a micromanipulator setup and electron-hardening adhesive to isolate and remove individual particles before synchrotron radiation analysis. This system allows for a greater range of new and existing analytical techniques, at increased detail and speed, to be applied to the material. Using this method, it was possible to erform detailed energy dispersive spectroscopy and synchrotron radiation characterisation of material likely ejected from the Fukushima Daiichi Nuclear Power Plant found within a sediment sample collected from the edge of the 30 km exclusion zone. Particulate material sub-micron in maximum dimension examined during this work via energy dispersive spectroscopy was observed to contain uranium at levels between 19.68 and 28.35 weight percent, with the application of synchrotron radiation spectroscopy confirming its presence as a major constituent.

With great effort and cost being devoted to the remediation of significant areas of eastern Japan affected by the incident, it is crucial to gain the greatest possible understanding of the nature of this contamination in order to inform the most appropriate clean-up response.

1. Introduction

The incident at the Fukushima Daiichi Nuclear Power Plant (FDNPP) beginning on the 11th of March 2011, after the magnitude 9.0 Tohoku-Oki earthquake and ensuing tsunami [1], is only the second ever event to be rated at Level 7, a major incident, on the International Nuclear Event Scale (INES) [2]. Following the disaster, material with an estimated activity of 340–800PBq [3–6] was released into the environment, with approximately 80% of ejected material transported eastwards out into the neighbouring Pacific Ocean [7,8]. Most of this activity was due to radionuclides of the elements Cs, Sr, I, Te, Kr and Xe; however comparatively little research, post-incident, has focused on the presence and environmental fate of the longer-lived, less volatile species such as U, Am and Pu [9,10].

The earliest forensic examination of radioactive emissions resulting from a nuclear material release occurred after nuclear testing in the United States amidst the Cold War [11,12]. Subsequently, the particulate releases from the nuclear accident at Chernobyl in 1986 were extensively studied with available techniques. Aerosol and sediment samples from the periphery of the plant and also from distal regions were sampled, with individual "hot particles" located using basic autoradiography [13,14], and their isotopic composition quantified using gamma-spectrometry [13,15,16].

The ex-situ removal and examination of individual particles, rather than the bulk material, were carried out on simulated radioactive fallout material by Shinonaga et al. [17] and Esaka et al. [18]. Quartz and glass needles with a diameter of 1 mm were sputter coated with gold and carbon before being attached to a micro-manipulator system installed within a scanning electron microscope (SEM) to isolate micron-scale particles. Additional work by Shinonaga et al. [19] used this same technique to analyse fragments of material originating from the nuclear weapon accident at Palomares, Spain in 1966. More recent work by

* Corresponding author. Tel.: +44 117 33 17686.
E-mail address: peter.martin@bristol.ac.uk (P.G. Martin).

http://dx.doi.org/10.1016/j.sab.2015.12.010

Kraiem et al. [20,21] and Park et al. [22] utilised an SEM with manipulator systems to extract particles for analysis using thermal ionisation mass spectrometry (TIMS), with Esaka et al. [23] using fission track analysis prior to particle removal and individual particle study also using TIMS.

Post Fukushima, primary work on the physical and chemical nature of radioactive particulate material collected 172 km southwest of the plant, was conducted by Adachi et al. [24] using airborne samples collected on quartz fibre filters at the Meteorological Research Institute (MRI), Tsukuba, Japan. Prior to their energy dispersive spectroscopy (EDS) analysis, individual micron sized particles were first identified using multi-step autoradiography with an Imaging Plate (IP), before the filter material was manually sectioned into smaller and smaller fragments; and ultimately deposited onto a glass substrate using a carbon cement. These spherical particles composed primarily of caesium were then analysed using synchrotron radiation x-rays [25] to reveal an internal core of uranium, in addition to thirteen other elements including zinc, barium and tin. The existence of the U-L_3 absorption edge at 17,166 eV was used to provide definitive confirmation for the presence of uranium.

To date, "hot particle" work has centred on aerosols collected via air-sampling systems within Japan [25,26] or further afield [8]. Important to the remediation and long term safety of the region is the accurate determination of not only the species present in the ground surface, but also their evolving size, distribution, solubility and mobility within the various affected river basin catchments e.g. Abukuma [27]. This knowledge will also facilitate a greater understanding as to the state of the four nuclear reactors at the time of each of the explosive releases.

As in previous works, here we focus on the detection of particles under an SEM via EDS, but instead sampling material from the bulk sediment. However, to improve the quality of compositional analysis performed on these individual sub-micron scale particles, a method to extract them from the surrounding bulk is discussed. Similar to work conducted by Abe et al. [25], confirmation of results achieved via EDS is performed using synchrotron radiation microfocus spectroscopy.

2. Method

2.1. Sampling and preparation

Roadside surface sediment samples were collected with permission of the local mayor during fieldwork in May 2014 from Iitate Village (3736.868N, 14042.503E), approximately 35 km northwest of the FDNPP. The material consisted of a fine-grained (<4 mm) soil mass with a proportion of coarser organic fragments such as leaf debris and plant material (up to 6 mm) as well as angular quartz grains (1–2 mm).

Approximately 0.1 g of sample material featuring all three of these components was placed across the surface of a large adhesive carbon disc (Leit tab). This mounting medium was selected due to its adhesive properties, but predominantly due to its low atomic (Z) number—exhibiting a low backscattered electron co-efficient.

2.2. Particle location

A scanning electron microscope (Zeiss Sigma™ Variable Pressure FE-SEM) (Oberkochen, Germany) equipped with a backscattered electron (Carl Zeiss AsB) and variable pressure secondary electron (Carl Zeiss VPSE-G3) detectors were used to perform the initial microscope observations. Manually scanning regions in a grid pattern, particles of interest would appear bright using the backscattered electron detector, in high contrast to the dark greys and blacks (low backscattered electron yield) exhibited by the soil and the adhesive carbon disk; both of which possess a lower atomic mass and backscatter coefficient. These probable emission particles were then compositionally analysed in-situ via EDS.

To negate the impact of charging on the samples due to their non-conductive nature, the variable pressure (VP) function of the instrument was utilised for locating material—introducing a nitrogen rich atmosphere in comparatively low vacuum (0.35–1.0 mbar) conditions.

2.3. Energy dispersive spectroscopy (EDS)

An Octane Plus™ Energy Dispersive Spectroscopy (EDS) system from EDAX™ (Mahwah, New Jersey, USA) provided point analysis and elemental mapping results of elemental composition, at an accelerating voltage of 20 kV, using a 120 μm beam aperture and 100 μA filament current in high current mode, verifying the presence or absence of actinide material at weight percent concentrations. A region comprising at least two thirds of the particle was rastered by the electron beam for elemental quantification for a period of 500 s. Maps of elemental abundance were obtained over an area including the particle in addition to the surrounding sediment to provide contrasting composition.

2.4. Particle removal

Removal of identified particles, each sub-micron in maximum dimension, was performed within an FEI™ Helios NanoLab™ 600 dual FIB-SEM system (Hillsboro, Oregon, USA), using a door mounted MM3A-Micromanipulator from Kleindiek Nanotechnik GmbH (Reutlingen, Germany) (Fig. 1). The piezo-electric based manipulator with minimum lateral, vertical and extension/retraction steps of 5, 3.5 and 0.5 nm respectively along with 360° rotation controlled a 100 nm tip tungsten needle (Picoprobe, GGB Industries, Naples, FL). Prior to its use, a focused ion beam (FIB) system was used to thin the needle to the smallest diameter tip possible. Without the variable pressure charge neutralisation function within the FEI™ instrument, a thin (approximately 2 nm) layer of gold was sputtered onto the samples surface using an Edwards™ Scancoat™ system.

An electron-beam hardening adhesive; SEMGlu™ by Kleindiek Nanotechnik GmbH [28], prevented the need for depositing platinum via beam assisted decomposition of a gaseous organo-metallic precursor (Trimethyl-methylcylopentadienyl Platinum-IV), commonly used as an adhesive within FIB/SEM systems. To prevent against the adhesive hardening prematurely, a low (0.17 nA) beam current and accelerating voltage (10 kV) were used. After locating the same region and particle of interest within the second instrument (Fig. 2a), storing its position within the control software, the sample stage was repositioned and a small quantity of the adhesive substance was applied to the very end of the tungsten needle of the manipulator within the microscope by progressively lowering and extending the needle until contacting with

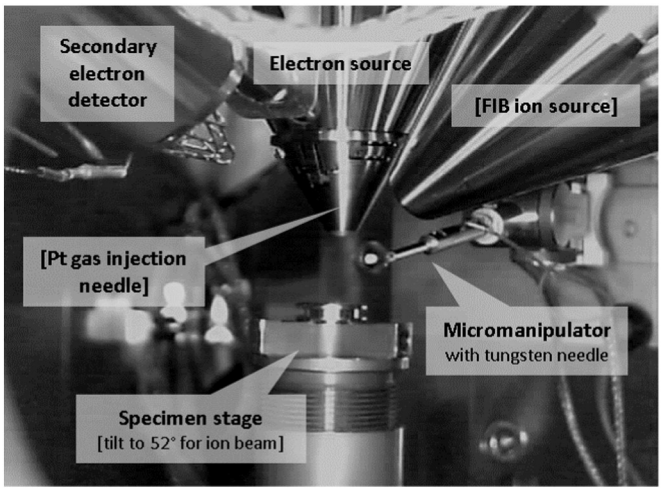

Fig. 1. Experimental layout of the FEI™ Helios NanoLab™ 600 dual FIB-SEM with Kleindiek™ MM3A-micromanipulator used for particle removal.

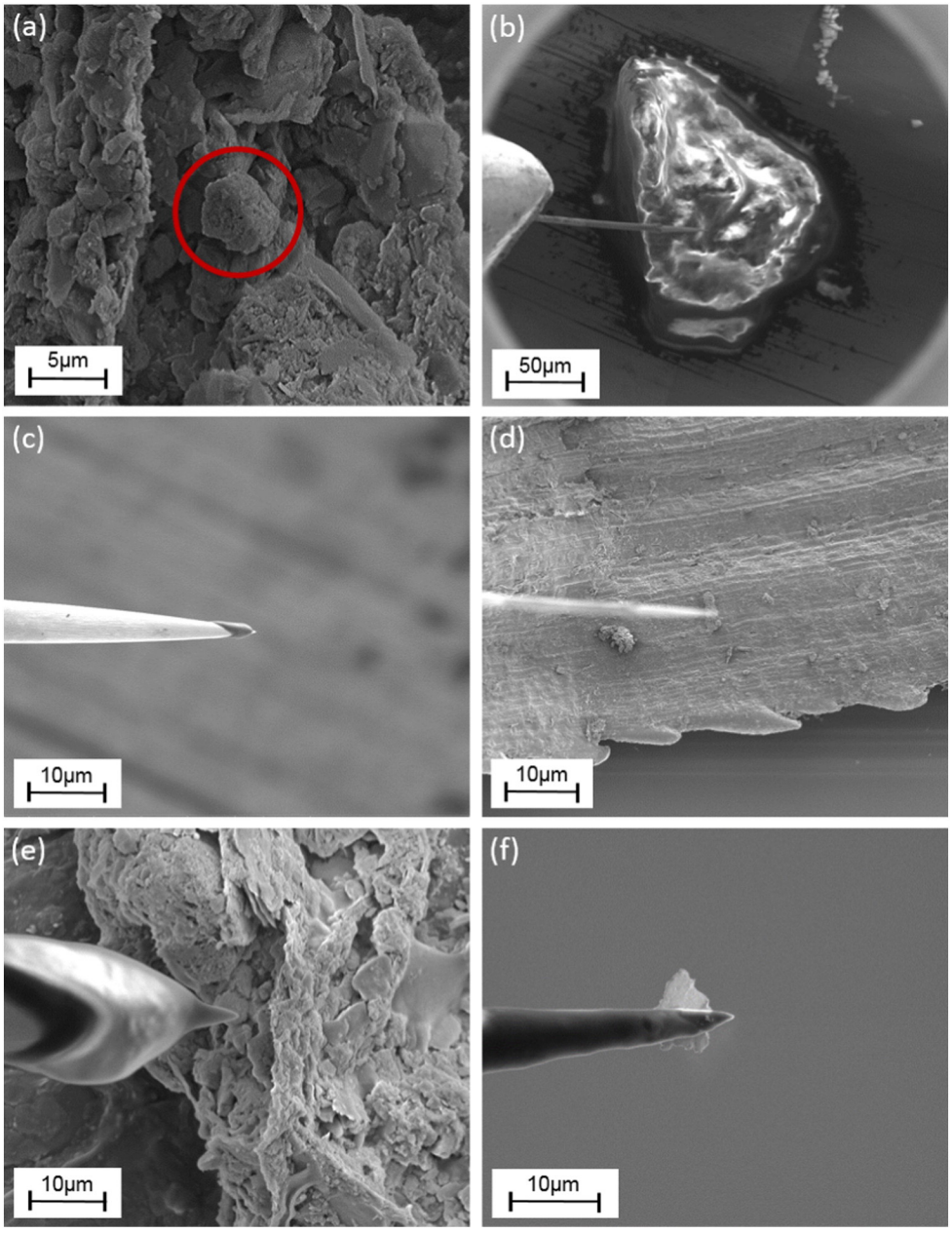

Fig. 2. Steps detailing the removal of a particle from sediment material; (a) locating particle using backscattered electrons and EDS, (b) and (c) applying a small quantity of SEMGlu™ to the tip of the tungsten needle in the instrument, (d) and (e) progressively bringing the needle into contact with the particle and (f) lifting out a Nd containing particle from the surrounding material, attached to the needle.

the glue (Fig. 2b). With the tip now prepared for the particle removal (Fig. 2c) the needle was then raised and retracted to position it clear above the sample. The stage was then returned back to the location of the particle to be removed (Fig. 2d). Following progressively lowering and extending the needle in a series of steps identical to those performed to collect the glue, the needle was slowly brought into contact with the particle (Fig. 2e), with an increase in the beam-current (from 0.17 to 1.4 nA) and magnification (to 50,000×) over the needles tip causing polymerisation and strong adhesion of the needle to the particle (Fig. 2f). The adhesive, composed entirely of low atomic number elements did not introduce metallic platinum to the particle, as would be the case when using platinum gas adhesion typically employed within FIB systems. Particles extracted from the sediment were left adhered to the tips for subsequent analysis.

2.5. Synchrotron data collection

Microfocus spectroscopy of particles adhered to the tips of tungsten needles was conducted on beamline I18 at Diamond Light Source (DLS), Harwell (UK) [29]. As a medium energy synchrotron, DLS has a storage ring with orbiting electrons at 3 GeV, and at the time of the experiment was operating with a beam current of 300 mA. The energy range producible by the I18 beamline is 2.05 to 20.05 keV.

The samples were placed individually on a three-axis high-precision controllable rotational stage (Thorlabs Inc., NJ, USA) for the experiment. The incident synchrotron beam energy was tuned using a cryogenically cooled Si [111] monochromator and subsequently focused down to a 2 × 2 μm spot using the silicon stripe on a pair of Kirkpatrick–Baez mirrors, which also provided requisite harmonic rejection. Throughout

all sample analyses, a consistent beam, sample and detector geometry was maintained; with the fluorescence detector mounted at 90° to the incident beam and needle-mounted sample positioned at 45° to the beam to ensure optimum collection conditions. A camera mounted within the experimental setup next to the stage provided visual assistance with the positioning of the sample for analysis.

To ensure that the heating effects produced by the X-ray beam on the sample did not cause the glue to fail or particle becoming dislodged; which would result in the radioactive sample falling into the beamline apparatus, a sealed transparent plastic sample bag was secured over the needle.

Needle-mounted samples were initially mapped using micro X-ray fluorescence (μ-XRF) to identify the correct position from which to subsequently obtain the micro-X-ray absorption near edge structure (μ-XANES) data. A six element SGX Sensortech Si Drift fluorescence detector (Xspress 3) (Chelmsford, Essex, UK) was used. Saturation effects on this detector were reduced by the insertion of a 0.1 mm Al foil, which also served to screen out lower energy absorption peaks. The fluorescence maps were collected at an energy of 18,100 eV—above the studied U-L_3 edge at 17,166 eV with a dwell of 30 s per point. Other edge energies at 115,602 eV (K), 21,756 eV (L_1) and 20,947 eV (L_2) all exist above

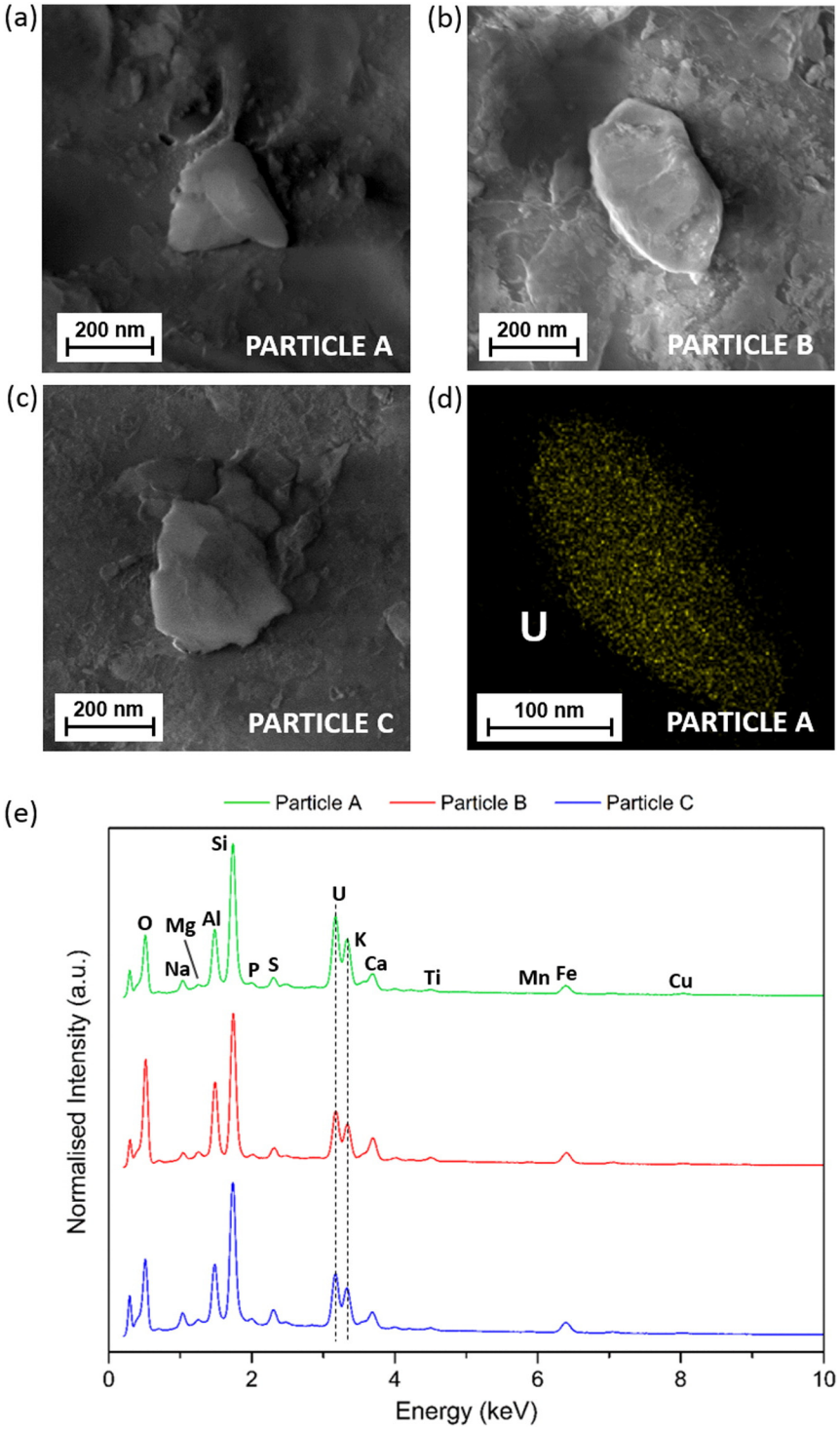

Fig. 3. (a), (b) and (c) SEM images of particles A, B and C respectively, (d) EDS uranium elemental map of particle A and (e) EDS spectra of each of the particles A, B and C with peaks identified, compositional results are presented within Table 1.

those possible on the beamline. Interpretation of fluorescence data was conducted using Python multichannel analyser (PyMCA) [30].

Subsequent collection of μ-XANES data was conducted at the identified point, pre-edge data was collected at 5 eV steps from 17,014 to 17,139 eV, with the main absorption peak collected at 0.5 eV steps to 17,200 eV, before then coarsening to 1.0 eV from 17,300 eV to the upper limit at 17,412 eV. For XANES scans of the sample, three scans of the same point were conducted for noise reduction through averaging. An identical apparatus setup was employed for the collection of XANES data to the previously collected μ-XRF.

2.6. Synchrotron data analysis

Processing of data acquired from I18 at Diamond Light Source including normalisation and linear combination fitting was performed with the Demeter package (version 0.9.21) of software [31], including Athena and Artemis based on the open source IFEFFIT code [32,33].

3. Results & discussion

3.1. Electron microscopy and energy dispersive spectroscopy

The results of SEM imaging of the three particles (A, B and C) are shown in Fig. 3 (a, b and c). Each particle was c. 200–500 nm in the longest dimension, with a sub-rounded to angular morphology. Results from the corresponding EDS analysis of the three particles are shown in Fig. 3 (e) with compositional analysis in Table 1. Each produced a near identical spectra of elemental composition; comprising a uranium component in addition to other lighter elements including; iron, silicon, aluminium, magnesium, phosphorus, sulphur and copper as well as oxygen and a trace amount of titanium. Much of the light element (e.g. Si, Al, C and O) signal occurring at low energies within these EDS spectra could be attributed to either the underlying material substrate or the particle.

These three particle compositions obtained via EDS, exhibit a strong compositional similarity to the central portion of the micron-scale particles analysed by Abe et al. [25], collected 172 km away from the FDNPP in Tsukuba. Although containing the volatile fission product element caesium at weight percent levels, unlike those examined here, the remaining elements observed within particles A, B and C of this work all exist as constituents of particles of those examined be Abe.

3.2. Particle removal

From a sample known to contain fragments of radiological material; initial location and subsequent removal within the SEM required approximately 1 h/particle—a marked increase in efficiency over other previously mentioned, widely employed methods. Hence, within one session, a considerable quantity of “hot” particles can be retrieved from the surrounding material for examination utilising a range of analytical techniques.

Having removed the sample from the surrounding sediment, the analysis conducted on the individual particles does not contain compositional information relating to the bulk—allowing for a much more accurate determination of composition.

As previously discussed, the application of SEMGlu™ over gaseous organo-metallic platinum does not introduce metallic species into the samples, which might present complications through isobaric interferences with techniques such as ICP-MS. For the attachment of material to the tungsten needles, SEMGlu™ also exhibits better physical properties than platinum. Unlike platinum, SEMGlu™ possesses a greater bond strength at 2 mN (Kleindiek Nanotechnik GmbH) and plasticity, to remain bonded to the needle [34].

Table 1
Calculated EDS elemental compositions of the three particles (A, B and C) examined during this study. Quantifications were conducted on the particles post removal from the sediment substrate to eliminate potential background interference.

Element	Weight percent		
	Particle A	Particle B	Particle C
O	26.66	36.44	29.88
Na	1.53	1.39	2.86
Mg	0.08	0.16	0.74
Al	7.82	8.99	8.09
Si	18.74	15.59	17.68
P	1.26	1.08	2.07
S	1.79	2.02	3.04
U	31.45	17.33	23.01
K	–	–	1.12
Ca	4.38	6.77	4.44
Ti	0.43	–	0.54
Mn	0.14	–	0.25
Fe	4.44	9.35	2.76
Cu	1.28	0.89	0.92

3.3. Synchrotron radiation μ-XANES

Confirmation of the presence of uranium via synchrotron radiation-μ-XANES is shown in Fig. 4. A clear peak at 17,166 eV corresponding to the U-L_3 edge is observed for each of the three particles A, B and C. These results verify those obtained via EDS, that uranium is present as a

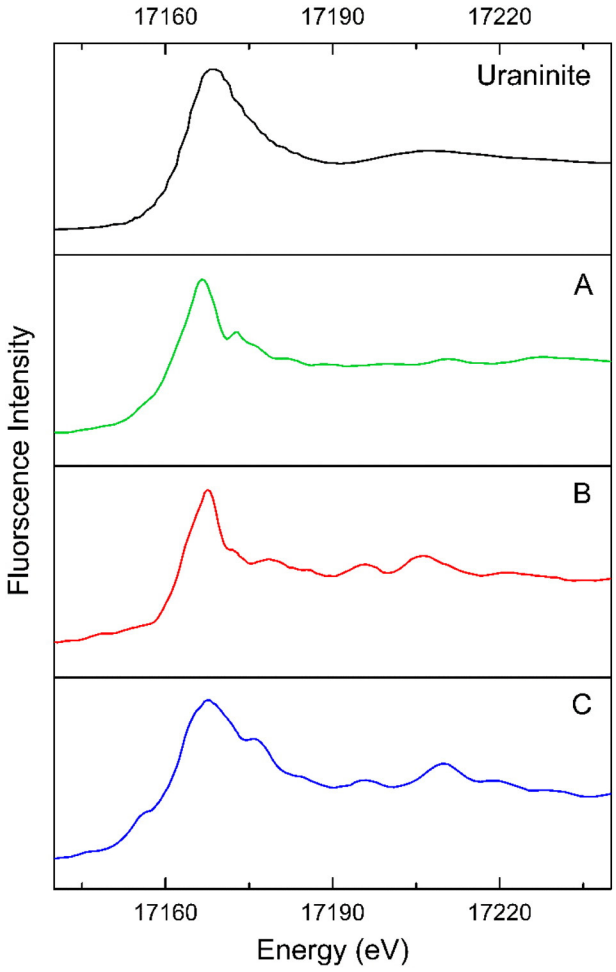

Fig. 4. Results of μ-XANES analysis of particles A, B and C at the uranium L_3 edge demonstrating the presence of uranium in all three particles. A reference spectra for uraninite (UO_2) is shown for comparison.

measurable constituent in particles found within sediment material collected near to the FDNPP.

Synchrotron analysis work by Abe et al. 2014 highlighted the existence of uranium at the centre of emission particles enclosed within a rind, containing amongst other elements the volatile fission product caesium, collected on filters some distance from the plant. The size of the uranium material contained within the spherical aerosol particles is consistent with that measured in this study. This similarity in the size of the uranium material may suggest that these particles share a common origin and are related to the same release event at the Fukushima plant.

4. Conclusions & future work

The use of micromanipulators for the removal of radioactive particles from contaminated material has here, as well as previously, presented a method of both heightened efficiency as well as greater resolution over traditionally employed methods. Results from this study have confirmed via two methods the presence of uranium within sediment samples collected at approximately 30 km along the main north-west trending fallout plume produced by the incident at Fukushima. The size of these particles is consistent with those reported by Adachi et al. [24], Abe et al. [25] and Malá et al. [35], suggesting a common provenance from the Fukushima Daiichi Nuclear Power Plant. Using synchrotron radiation, it has been possible to confirm the presence of uranium via non-destructive means, preserving valuable samples for subsequent methods.

Due to the high thermal effects imparted onto the sample via the incident X-ray beam, difficulties were experienced whereby the poor thermal conductivity of the tungsten needle onto which the particle was mounted thermally drifted, in some instances by several microns over the course of the experiment. To prevent against this, and the potential issue of sample oxidation within the beam, samples analysed during future work will be enclosed within an envelope made from Kapton™ film, flushed continually with an inert gas such as nitrogen or argon.

Future work will undertake more quantitative compositional analysis via techniques such as inductively coupled plasma mass-spectrometry (ICP-MS), Raman Spectroscopy or Atom Probe; with internal structure being evaluated through transmission electron microscopy (TEM) or electron backscattered diffraction (EBSD).

Keeping the particle attached to the tip of the tungsten needle and progressively thinning using the instruments ion-beam, it is possible to prepare a thin foil of such a fallout particle for TEM analysis. By applying additional SEMGlu™ to the underside of particles whilst still adhered to the needle, extracted samples can then be placed onto a substrate (such as a piece of silicon wafer) which can then be dissolved to undertake particle specific mass spectrometry compositional analysis.

Over previous methods, where high levels of background are present due to the existence of a substrate material, the isolation of individual particles ensures that accurate analysis is conducted exclusively on the material of interest. This becomes of significant importance for isotopic studies, whereby background contamination can be eliminated. The recent installation of a micromanipulator setup within the Zeiss Sigma™ FE-SEM will prevent the need for sample transfer between instruments as well as the requirement for a conductive gold-coating to be applied for charge neutralisation that would otherwise contribute to background analytical noise during subsequent analysis. Due to the large number of electron microscopes in analytical laboratories worldwide, most of which are fitted with EDS systems, the uptake of this method for the analysis of samples is both simple and cost-efficient.

Upcoming fieldwork within Fukushima Prefecture will seek to sample sites closer to the release event at the plant on the eastern coast. It is hoped that these samples will allow for additional work to be performed to characterise any variation in uranium size distribution with distance to from the plant.

Acknowledgements

The authors wish to thank Diamond Light Source for access to beamline I18 (SP13138) that contributed to the results presented here.

References

[1] M. Simons, S.E. Minson, A. Sladen, F. Ortega, J. Jiang, S.E. Owen, et al., The 2011 magnitude 9.0 Tohoku-Oki earthquake: mosaicking the megathrust from seconds to centuries, Science 332 (2011) 1421–1425, http://dx.doi.org/10.1126/science.1206731.
[2] IAEA, The International Nuclear and Radiological Event Scale User's Manual, International Atomic Energy Agency, Vienna, Austria, 2008 (http://www-pub.iaea.org/MTCD/Publications/PDF/INES2013web.pdf).
[3] G. Steinhauser, A. Brandl, T.E. Johnson, Comparison of the Chernobyl and Fukushima nuclear accidents: a review of the environmental impacts, Sci. Total Environ. 470-471 (2014) 800–817, http://dx.doi.org/10.1016/j.scitotenv.2013.10.029.
[4] N. Hamada, H. Ogino, Food safety regulations: what we learned from the Fukushima nuclear accident, J. Environ. Radioact. 111 (2012) 83–99, http://dx.doi.org/10.1016/j.jenvrad.2011.08.008.
[5] J.E. Ten Hoeve, M.Z. Jacobson, Worldwide health effects of the Fukushima Daiichi nuclear accident, Energy Environ. Sci. 5 (2012) 8743, http://dx.doi.org/10.1039/c2ee22019a.
[6] V. Winiarek, M. Bocquet, O. Saunier, A. Mathieu, Estimation of errors in the inverse modeling of accidental release of atmospheric pollutant: application to the reconstruction of the cesium-137 and iodine-131 source terms from the Fukushima Daiichi power plant, J. Geophys. Res. 117 (2012), D05122http://dx.doi.org/10.1029/2011JD016932.
[7] N. Yoshida, J. Kanda, Geochemistry. Tracking the Fukushima radionuclides, Science 336 (2012) 1115–1116, http://dx.doi.org/10.1126/science.1219493.
[8] O. Masson, A. Baeza, J. Bieringer, K. Brudecki, S. Bucci, M. Cappai, et al., Tracking of airborne radionuclides from the damaged Fukushima Dai-ichi nuclear reactors by European networks, Environ. Sci. Technol. 45 (2011) 7670–7677, http://dx.doi.org/10.1021/es2017158.
[9] A. Sakaguichi, A. Kadokura, P. Steier, K. Tanaka, Y. Takahashi, H. Chiga, et al., Isotopic determination of U, Pu and Cs in environmental waters following the Fukushima Daiichi Nuclear Power Plant accident, Geochem. J. 46 (2012) 355–360, http://dx.doi.org/10.2343/geochemj.2.0216.
[10] J. Zheng, K. Tagami, Y. Watanabe, S. Uchida, T. Aono, N. Ishii, et al., Isotopic evidence of plutonium release into the environment from the Fukushima DNPP accident, Sci. Rep. 2 (2012) 304, http://dx.doi.org/10.1038/srep00304.
[11] C.E. Adams, N.H. Farlow, W.R. Schell, The compositions, structures and origins of radioactive fall-out particles, Geochim. Cosmochim. Acta 18 (1960) 42–56, http://dx.doi.org/10.1016/0016-7037(60)90016-8.
[12] J. Mackin, P. Zigman, D. Love, D. Macdonald, D. Sam, Radiochemical analysis of individual fall-out particles, J. Inorg. Nucl. Chem. 15 (1960) 20–36, http://dx.doi.org/10.1016/0022-1902(60)80005-X.
[13] L. Devell, H. Tovedal, U. Bergström, A. Appelgren, J. Chyssler, L. Andersson, Initial observations of fallout from the reactor accident at Chernobyl, Nature 321 (1986) 192–193, http://dx.doi.org/10.1038/321192a0.
[14] T. Raunemaa, S. Lehtinen, H. Saari, M. Kulmala, 2–10 μm sized hot particles in chernobyl fallout to Finland, J. Aerosol Sci. 18 (1987) 693–696, http://dx.doi.org/10.1016/0021-8502(87)90099-1.
[15] R. Broda, Gamma spectroscopy analysis of hot particles from the Chernobyl fallout, http://www.iaea.org/inis/collection/NCLCollectionStore/_Public/21/014/21014068.pdf1986 (accessed September 3, 2014).
[16] I. Balásházy, G. Szabadyné-Szende, M. Lorinc, P. Zombori, Gamma-spectrometric examination of hot particles emitted during the Chernobyl accident, KFKI Prepr. 1987-24/K, 1987.
[17] T. Shinonaga, D. Donohue, D. Klose, T. Kuno, Y. Kuno, F. Esaka, et al., Particle-chemical analysis of uranium and plutonium, Symp. Int. Safeguards Addressing Verif. Challenges, 2006 (http://www-pub.iaea.org/MTCD/publications/PDF/P1298/P1298_Contributed_Papers.pdf.
[18] F. Esaka, K.T. Esaka, C.G. Lee, M. Magara, S. Sakurai, S. Usuda, et al., Particle isolation for analysis of uranium minor isotopes in individual particles by secondary ion mass spectrometry, Talanta 71 (2007) 1011–1015, http://dx.doi.org/10.1016/j.talanta.2006.05.091.
[19] T. Shinonaga, F. Esaka, M. Magara, D. Klose, D. Donohue, Isotopic analysis of single uranium and plutonium particles by chemical treatment and mass spectrometry, Spectrochim. Acta Part B 63 (2008) 1324–1328, http://dx.doi.org/10.1016/j.sab.2008.09.001.
[20] M. Kraiem, S. Richter, H. Kühn, Y. Aregbe, Development of an improved method to perform single particle analysis by TIMS for nuclear safeguards, Anal. Chim. Acta 688 (2011) 1–7, http://dx.doi.org/10.1016/j.aca.2010.12.003.
[21] M. Kraiem, S. Richter, H. Kühn, E.A. Stefaniak, G. Kerckhove, J. Truyens, et al., Investigation of uranium isotopic signatures in real-life particles from a nuclear facility by thermal ionization mass spectrometry, Anal. Chem. 83 (2011) 3011–3016, http://dx.doi.org/10.1021/ac103153k.
[22] J.-H. Park, S. Park, K. Song, Isotopic analysis of NUSIMEP-6 uranium particles using SEM-TIMS, Mass Spectrom. Lett. 4 (2013) 51–54, http://dx.doi.org/10.5478/MSL.2013.4.3.51.
[23] F. Esaka, D. Suzuki, M. Magara, Identifying uranium particles using fission tracks and microsampling individual particles for analysis using thermal ionization mass spectrometry, Anal. Chem. 87 (2015) 3107–3113, http://dx.doi.org/10.1021/acs.analchem.5b00236.

[24] K. Adachi, M. Kajino, Y. Zaizen, Y. Igarashi, Emission of spherical cesium-bearing particles from an early stage of the Fukushima nuclear accident, Sci. Rep. 3 (2013) 2554, http://dx.doi.org/10.1038/srep02554.
[25] Y. Abe, Y. Iizawa, Y. Terada, K. Adachi, Y. Igarashi, I. Nakai, Detection of uranium and chemical state analysis of individual radioactive microparticles emitted from the Fukushima nuclear accident using multiple synchrotron radiation X-ray analyses, Anal. Chem. 86 (2014) 8521–8525, http://dx.doi.org/10.1021/ac501998d.
[26] H. Mukai, T. Hatta, H. Kitazawa, H. Yamada, T. Yaita, T. Kogure, Speciation of radioactive soil particles in the Fukushima contaminated area by IP autoradiography and microanalyses, Environ. Sci. Technol. (2014)http://dx.doi.org/10.1021/es502849e.
[27] Y. Yamashiki, Y. Onda, H.G. Smith, W.H. Blake, T. Wakahara, Y. Igarashi, et al., Initial flux of sediment-associated radiocesium to the ocean from the largest river impacted by Fukushima Daiichi Nuclear Power Plant, Sci. Rep. 4 (2014) 3714, http://dx.doi.org/10.1038/srep03714.
[28] S. Kleindiek, A. Rummel, K. Schock, E-beam hardening SEM glue for fixation of small objects in the SEM, http://link.springer.com/chapter/10.1007/978-3-540-85156-1_2832008.
[29] J.F.W. Mosselmans, P.D. Quinn, A.J. Dent, S.A. Cavill, S.D. Moreno, A. Peach, et al., I18—the microfocus spectroscopy beamline at the Diamond Light Source, J. Synchrotron Radiat. 16 (2009) 818–824, http://dx.doi.org/10.1107/S0909049509032282.
[30] V.A. Solé, E. Papillon, M. Cotte, P. Walter, J. Susini, A multiplatform code for the analysis of energy-dispersive X-ray fluorescence spectra, Spectrochim. Acta Part B 62 (2007) 63–68, http://dx.doi.org/10.1016/j.sab.2006.12.002.
[31] B. Ravel, M. Newville, ATHENA, ARTEMIS, HEPHAESTUS: data analysis for X-ray absorption spectroscopy using IFEFFIT, J. Synchrotron Radiat. 12 (2005) 537–541, http://dx.doi.org/10.1107/S0909049505012719.
[32] J.J. Rehr, R.C. Albers, S.I. Zabinsky, High-order multiple-scattering calculations of x-ray-absorption fine structure, Phys. Rev. Lett. 69 (1992) 3397–3400, http://dx.doi.org/10.1103/PhysRevLett.69.3397.
[33] M. Newville, IFEFFIT: interactive XAFS analysis and FEFF fitting, J. Synchrotron Radiat. 8 (2001) 322–324, http://dx.doi.org/10.1107/S0909049500016964.
[34] Kleindiek Nanotechnik GmbH, SEMGlu Product Brochure, 9.04 (n.d.) 2. http://www.kleindiek.com/fileadmin/public/brochures/semglu.pdf (accessed September 26, 2015).
[35] H. Malá, P. Rulík, V. Bečková, J. Mihalík, M. Slezáková, Particle size distribution of radioactive aerosols after the Fukushima and the Chernobyl accidents, J. Environ. Radioact. 126 (2013) 92–98, http://dx.doi.org/10.1016/j.jenvrad.2013.07.016.